Photonic Cavity Synchronization of Nanomechanical Oscillators

Mahmood Bagheri,[1] Menno Poot,[1] Linran Fan,[1] Florian Marquardt,[2,3] and Hong X. Tang[1,*]

[1]*Department of Electrical Engineering, Yale University, New Haven, Connecticut 06511, USA*
[2]*Institute for Theoretical Physics II, Universität Erlangen-Nürnberg, Staudstraße 7, 91058 Erlangen, Germany*
[3]*Max Planck Institute for the Science of Light, Günther-Scharowsky-Straße 1/Bau 24, D-91058 Erlangen, Germany*

(Received 3 June 2013; revised manuscript received 8 October 2013; published 21 November 2013)

Synchronization in oscillatory systems is a frequent natural phenomenon and is becoming an important concept in modern physics. Nanomechanical resonators are ideal systems for studying synchronization due to their controllable oscillation properties and engineerable nonlinearities. Here we demonstrate synchronization of two nanomechanical oscillators via a photonic resonator, enabling optomechanical synchronization between mechanically isolated nanomechanical resonators. Optical backaction gives rise to both reactive and dissipative coupling of the mechanical resonators, leading to coherent oscillation and mutual locking of resonators with dynamics beyond the widely accepted phase oscillator (Kuramoto) model. In addition to the phase difference between the oscillators, also their amplitudes are coupled, resulting in the emergence of sidebands around the synchronized carrier signal.

DOI: 10.1103/PhysRevLett.111.213902 PACS numbers: 42.82.Et, 05.45.Xt, 07.10.Cm, 42.50.Wk

Synchronization is a ubiquitous phenomenon where the phase difference between free-running oscillators remains constant due to the mutual coupling. Besides its well-accepted importance in biological sciences, today synchronization is becoming a powerful tool for many engineered systems [1]. For instance, synchronization is desirable in situations where high oscillating power, strong coherence, or low phase noise are needed, such as lasers [2], phase-locked loops [3], Josephson junction arrays [4], and spin-torque resonators [5]. Synchronization also promises to improve the accuracy of time-keeping devices [6]. Since the observations of synchronization in pendulums [7] this concept has found its bearings in science and engineering due to its potential applications in generating low-noise stable oscillating signals. Nanomechanical oscillators, on the other hand, are very appealing as they simultaneously offer high quality factor resonances, excellent scalability [8,9] and are ideal systems for synchronization studies due to their highly engineerable nonlinearities [10].

However, achieving reproducible and strong coupling in nanomechanical devices remains difficult due to the unavoidable device nonuniformity and weak mutual coupling. This can be circumvented by coupling nanomechanical resonators to an optical cavity [11]. Recently, synchronization between two closely spaced micromechanical resonators was demonstrated using a hybrid optical mode of two coupled disk resonators and the synchronization phase space was predicted using the Kuramoto model [12]. Here we experimentally demonstrate the first synchronization of two spatially separated nanoscale radio-frequency oscillators integrated inside an optical racetrack cavity. We show that this leads to a limit cycle in the reduced three-dimensional mechanical phase space (the two mechanical resonators' amplitudes and their phase difference [13]) and that the dynamics of two mechanical modes coupled via a common optical mode cannot be captured by the standard Kuramoto model [14]: as a result of the additional degrees of freedom of the coupled system, slow dynamics appear on top of the limit cycle, and sidebands emerge. These sidebands are true signatures of synchronized motion in the mechanical domain and are not to be confused with simple nonlinear intermodulation oscillatory modes. Their presence is important for the phase noise performance of synchronized optomechanical oscillators, and could counteract the common perception that synchronized states should always improve phase noise performance.

We investigate the interaction between two nanomechanical resonators that are linked in an optical racetrack [Fig. 1(a)]; they are mechanically isolated, due to their large separation (~ 80 μm), ensuring that any coupling between them is through the optical field. The fabrication of these integrated photonic devices is readily scalable [15], making this an ideal platform for synchronization studies [11,14]. The silicon beams are slightly buckled [15] and they may end up in the up or down state [Fig. 1(a)].

The measurement setup shown in Fig. 1(d) consists of a strong pump laser to create cavity backaction and a weak probe to detect the motion [13]. When the two resonators are both in the buckled-up state [Fig. 1(b)] their resonance frequencies are close, with a small difference due to fabrication imperfections (6.53 vs 6.61 MHz). However, when one resonator is displaced from the up state to the down state, its mechanical resonance frequency drops to 4.05 MHz [Fig. 1(c)] due to asymmetries of the double-well potentials [13].

Single resonator optomechanical oscillators (OMOs) have been the subject of intense studies in recent years [16–18]. However, when multiple oscillators are embedded in a single cavity new phenomena will appear due to the

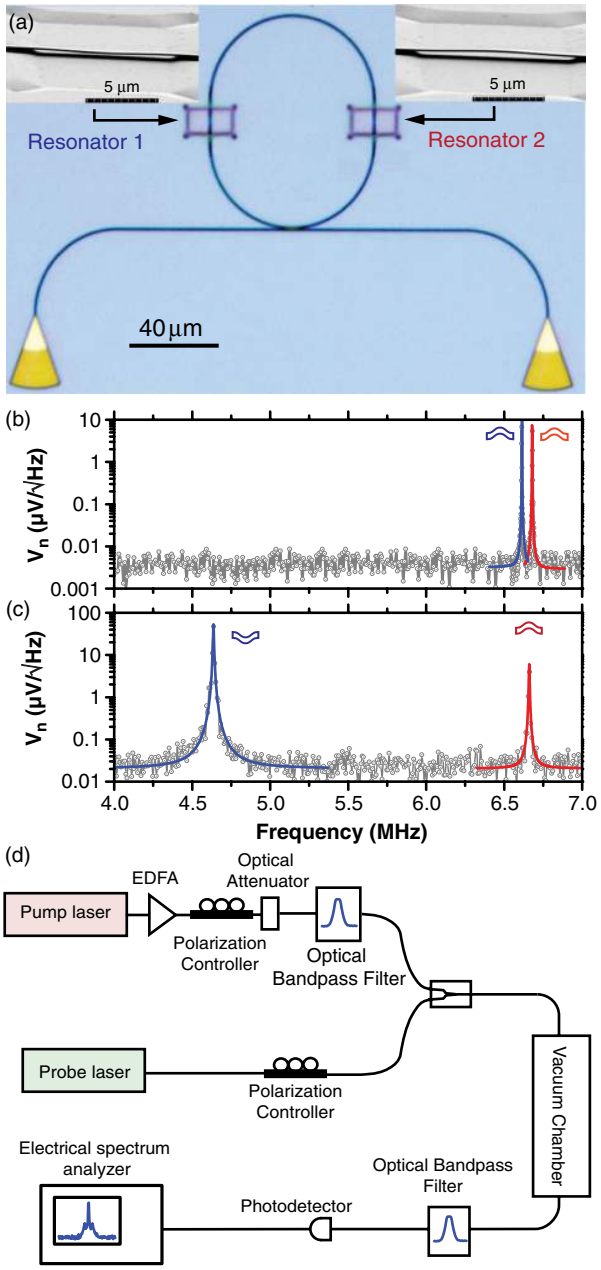

FIG. 1 (color online). (a) Micrograph of a racetrack cavity with two 110 nm × 500 nm × 10 μm suspended portions as nanomechanical resonators. Insets show scanning electron micrographs of the mechanical resonators in buckled down (left) and buckled up (right) state. (b),(c) thermal noise spectra in the up-up (b) down-up state (c). (d) The measurement setup with a weak probe laser, and a pump.

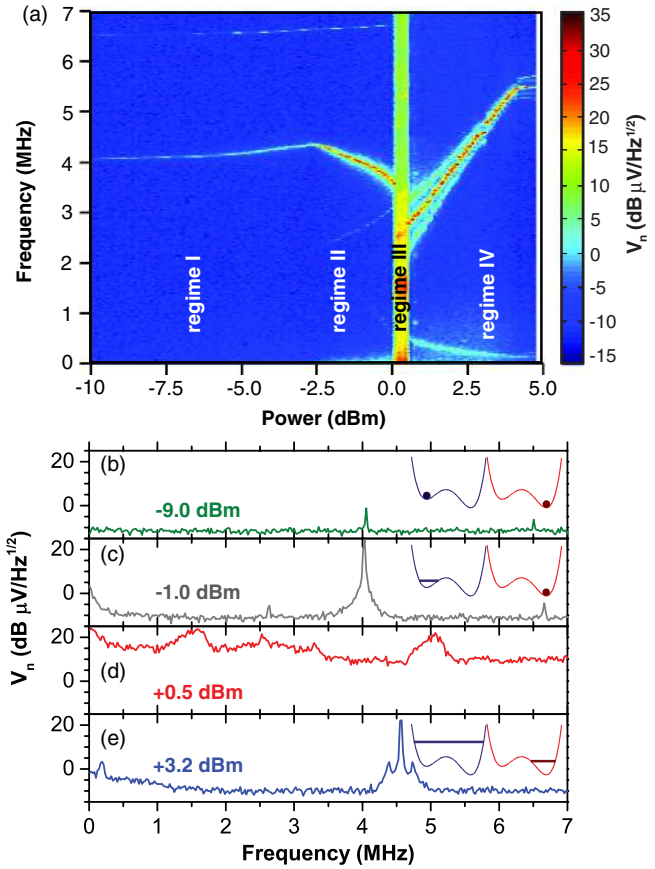

FIG. 2 (color online). (a) The evolution of the rf power spectrum of the transmitted light as the pump power increases. (b)–(e) Cuts through panel (a) at the indicated pump power when both resonators are in a thermal state regime I, (b); (c) one resonator is in thermal motion while the other resonator experiences regenerative oscillations (regime II); (d) the chaotic regime (III) and (e) the two resonators are synchronized (regime IV). The insets schematically show the energy of resonators 1 (left) and 2 (right); dots correspond to small thermal motion, and lines to large oscillations.

mutual coupling via the cavity field. Figure 2(a) displays the evolution of the rf power spectrum of the transmitted probe laser light (the pump laser is blue detuned at $\Delta_0/\kappa = 0.3$, where Δ_0 is the detuning between the laser and cavity frequency, and κ is the cavity linewidth). At the lowest pump powers the thermomechanical motion of each resonator is visible as two lines at 4.0 and 6.5 MHz, respectively. Upon increasing the pump power in this first regime, the backaction amplifies their Brownian motion. Also, the optical spring effect [19] is visible as an increase in the resonance frequencies. Both effects are stronger in the 4 MHz resonator since it is in the buckled down state [15]. The difference in backaction confirms that optical backaction is stronger than photothermal effects as the latter would be the same on both resonators [20].

When the pump is increased beyond −2.7 dBm, the optomechanical gain fully compensates the mechanical damping of the resonator with lower threshold, which we will label as "1", which starts to self-oscillate. This demarcates the onset of regime II, which ranges from −2.7 to 0.2 dBm. Yet, even though the oscillation amplitude of resonator 1 increased dramatically, the thermal motion of resonator 2 is undisturbed and is still clearly visible in Figs. 2(a) and 2(b). Note that the frequency difference between the two resonators (2.5 MHz) is much larger

than the spectral width of resonator 2, so the cavity occupation oscillation induced by OMO 1 cannot efficiently drive the other resonator. Regime II thus corresponds to the single oscillator system that we studied previously. One might expect that resonator 2 simply starts to oscillate when the power is increased beyond the second threshold which is higher due to its lower g_{om}. Instead, different dynamics is encountered (regime III) where the power spectrum displays a large magnitude over a wide range of frequencies. Here, the motion is chaotic and the phase, amplitude, and frequency of the transmitted probe light change on short time scales. This chaotic behavior only exists for a limited power range and vanishes beyond 0.7 dBm.

Above 0.7 dBm the two oscillators start their synchronized motion, as evidenced by a dramatic change in the mechanical displacement spectrum. In regime IV the detected photocurrent contains a strong narrow tone and, more importantly, the thermomechanical motion of resonator 2 is now no longer visible. The single strong peak in the RF spectrum indicates that both resonators are oscillating at the same frequency. We have thus synchronized the two resonators despite the extremely large frequency difference: the second mode, originally at 6.7 MHZ, was almost twice as fast as the oscillations of the first mode at 3.9 MHz, indicating the extremely strong optomechanical interactions and the tunability of the double-well potential in our system.

The spectra in regime IV also reveal another surprise: Sidebands emerge around the carrier peak. A close inspection of Figs. 2(a) and 2(e) shows that the spectra contain two equally spaced sidebands ~100–500 kHz from the carrier. Their presence implies a deteriorated signal phase noise at that particular sideband offset frequency [21]. These weak (~ 20–35 dBc), but clearly defined, sidebands are not transient phenomena as they persist during the entire data-acquisition time, which is much longer than the damping time of the resonator γ^{-1}. Also, in regime II [Fig. 2(c)] with only a single OMO present, sidebands are absent, ruling out low-frequency thermal instabilities [22] interfering with optomechanical oscillations.

To understand the origin of synchronization and the slow dynamics in the cavity-coupled oscillators, we theoretically analyze this system [13]. Multiple uncoupled oscillators will each oscillate at their own frequency, but the cavity field couples the oscillators enabling synchronization, as will be shown. When the frequency difference between the resonators $\upsilon \ll \bar{\Omega}$, the equations of motion for their complex amplitude $U_k = g_{om,k}\langle(u_k + \dot{u}_k/i\bar{\Omega}) \times \exp(-i\bar{\Omega}t)\rangle = A_k \exp(i\theta_k)$ in the frame rotating at the average frequency $\bar{\Omega} = \frac{1}{2}(\Omega_1 + \Omega_2)$ become [14,23,24]

$$\dot{U}_{1,2} = \pm i\frac{\upsilon}{2}U_{1,2} - \frac{\gamma_{1,2}}{2}U_{1,2} - i\bar{\Omega}c_{om,1,2}\Phi(t), \quad (1)$$

where u_k are the displacements of the two resonators ($k = 1, 2$) and $\Phi(t)$ describes how the photon occupation responds to a dynamic displacement [24]. $c_{om,k} = \hbar n_{\max} g_{om,k}^2/m_k\bar{\Omega}^3$ are the coupling strengths and $n_{\max}$ is the maximum number of photons in the cavity. The same reasoning as for a single OMO shows that for multiple resonators coupled to the same cavity the latter only feels their *combined* effect, and the cavity response is $\Phi(t) = \Phi[A_+(t)]$, where A_+ is the magnitude of the summed complex amplitudes $U_+(t) = \sum_k U_k(t) = A_+(t)\exp[i\theta_+(t)]$. A_+ depends on the phase difference between the individual oscillators, but not on the overall phase θ_+. The equations of motion for the two OMOs are thus coupled together via U_+ and the cavity response function $\Phi(A_+)$. Synchronization implies that they rotate at the same frequency $\bar{\Omega} + \epsilon$. Hence, $U_{1,2}(t) = Y_{1,2}\exp(i\epsilon t)$ must be a solution to Eq. (1): if no such solution exists, synchronization cannot take place. Inserting $U_{1,2}(t)$ into Eq. (1) yields

$$\Phi(A_+) = \frac{1}{\bar{\Omega}}\frac{(\frac{\upsilon}{2})^2 - \epsilon^2 + i\epsilon\bar{\gamma} + \frac{i\delta\gamma\upsilon}{4} + (\frac{\bar{\gamma}}{2})^2 - (\frac{\delta\gamma}{4})^2}{2\epsilon\bar{c}_{om} + \upsilon\frac{\delta c_{om}}{2} + i\frac{\delta c_{om}}{2}\frac{\delta\gamma}{2} - i\bar{\gamma}\bar{c}_{om}}, \quad (2)$$

where $\bar{c}_{om}$ (δc_{om}) and $\bar{\gamma}$ ($\delta\gamma$) are the average (difference in) coupling strengths and damping rates, respectively. Solving Eq. (2) is illustrated in Fig. 3(a); the left-hand side is a curve in the complex plane parameterized by A_+ (for a given detuning and decay rate), whereas the right hand side depends only on the oscillators' properties and is parameterized by the unknown frequency ϵ. Intersections of the two curves are thus solutions to Eq. (2). Equation (1) then gives the individual contributions Y_1 and Y_2 including their phases relative to the carrier $Y_+ = Y_1 + Y_2$. Figure 3(b) shows that they have a similar, but not identical, magnitude and oscillator 1 moves ahead of the second. Finally, for sufficiently asymmetric oscillators, the two curves can intersect more than once, leading to multistability [23,24], even in the unresolved sideband regime where a single oscillator always has a unique amplitude.

Equation (2) thus yields the fixed points with synchronization. However, to understand the dynamics around the corresponding limit cycle, Eq. (1) can be expanded for small excursions and the eigenvalues can be found. There are three independent degrees of freedom: the two oscillation amplitudes and the phase difference between them. The fourth degree of freedom, the overall phase θ_+, is not fixed, yielding a zero eigenvalue. Depending on the values of the other three eigenvalues, the coupled system can return to the fixed point with oscillations (underdamped). In this case, any displacement of an oscillator, e.g., due to the thermal force, will return back to the fixed point in an oscillatory fashion, which shows up as sidebands in the frequency domain. For a single oscillator the eigenvalue is real [24] and no sidebands appear as it overdampedly returns to the limit cycle.

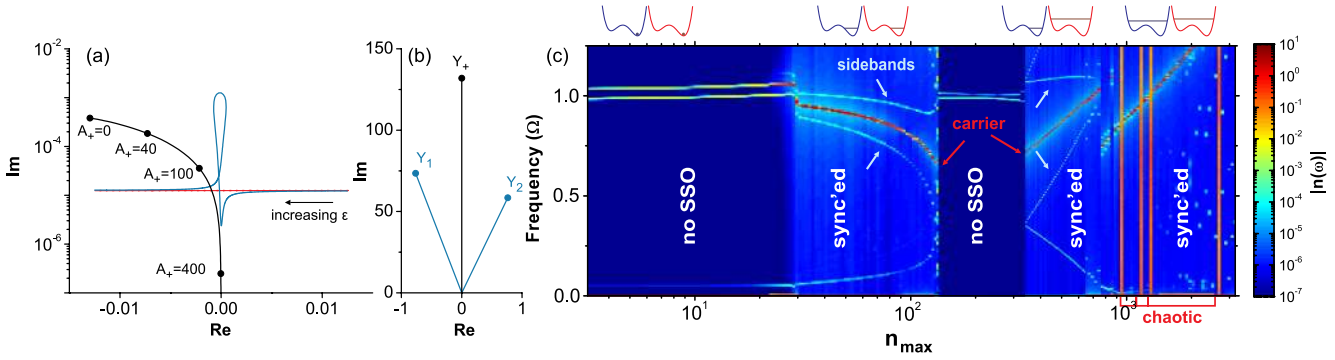

FIG. 3 (color online). (a) Complex plane representation of the cavity response $\Phi(A_+)$ (black) and the right-hand side of Eq. (5) for two identical oscillators (red) and two oscillators with $\bar{\gamma} = 0.001\ \bar{\Omega}$, $\bar{c}_{om} = 20$, $\upsilon = 0.01\ \bar{\Omega}$, $\delta\gamma = 0.0018\ \bar{\Omega}$, and $\delta c_{om} = 0$ (blue). The curves intersect at $A_+ = 132.0$ and $\epsilon = 0.0438\bar{\Omega}$ (b) Complex amplitudes of the individual oscillators for the solution shown in (a). (c) Color plot of the Fourier transform of the photon number on a logarithmic scale. The carrier tone and its sidebands are indicated by red and white arrows, respectively. The parameters are $Q_1 = Q_2 = 6000$, $\kappa = 526\bar{\Omega}$, $\Delta_0 = 0.493\kappa$, $g_{om,1} = g_{om,2} = 1$.

The analytical model thus hints that the observed sidebands are due to the thermal force noise acting on the oscillators. To further analyze the synchronization dynamics, the full equation of motion of the resonators and that of the cavity field are integrated numerically [with mechanical nonlinearities included, see Eqs. (S1) and (S2) in the Supplemental Material [13]]. We chose to simulate a conceptually clear situation with nearly identical resonators (5% frequency difference and identical g_{om}). The effect of force noise is accounted for by kicking the resonators away from their steady state oscillations (see the Supplemental Material [13] for a simulation with a stochastic force instead of kicks). Figure 3(c) shows the evolution of the light field power spectrum as a function of n_{max} (i.e., the pump power). Similar to the experiment (Fig. 2), at low power two weak upward-tuning peaks are visible. Around $n_{max} = 30$ the oscillations start, but now the two resonators immediately oscillate simultaneously [25]. As expected from our analytical theory of synchronized motion, sidebands appear in the spectrum, but only when force noise (i.e., kicks) is included. As illustrated in [13] the oscillators are truly phase locked in this regime, indicating full synchronization. When further increasing n_{max} the oscillations grow towards the top of the potential barriers and hence the frequency goes down. When the barrier is crossed at $n_{max} = 134$ the detuning suddenly changes dramatically and the oscillations stop. However, they reappear at higher powers and above the barrier, just as in the experiment, the oscillation frequency increases with increasing power [see also Fig. 2(a)]. Also note that the sidebands start out far from the carrier at the onset ($n_{max} = 335$) of the oscillations in this regime and that, just as in Fig. 2(a), they converge towards the carrier with increasing power. Also, the stochastic simulation [13] shows sideband strengths of the same magnitude as observed experimentally, confirming their thermal origin. Finally, the simulations also reproduce bands with chaotic behavior with broad spectrums similar to the one in Fig. 2(d). The simulations thus qualitatively reproduce most of the features observed in the experiment, including the correct tuning, the appearance of the sidebands of the synchronized resonators due to thermal force noise with the correct strength, and chaos.

We have also studied the dynamics of a single mechanical oscillator in the presence of an external oscillator encoded in the light field. This is extremely important in the context of synchronizing a remote oscillator to an external clock and also further validates our model for optomechanical synchronization. To this end, the pump power is set between the oscillation thresholds of the first and second resonator (so that the latter does not play a role) and is modulated at frequency $\Omega_0 = 6.800$ MHz. When the modulation index (m) is zero, resonator 1 oscillates freely in the up state at 6.804 MHz as shown in the bottom spectrum in Fig. 4. However, when the modulation is switched on the oscillations jump to Ω_0, synchronizing

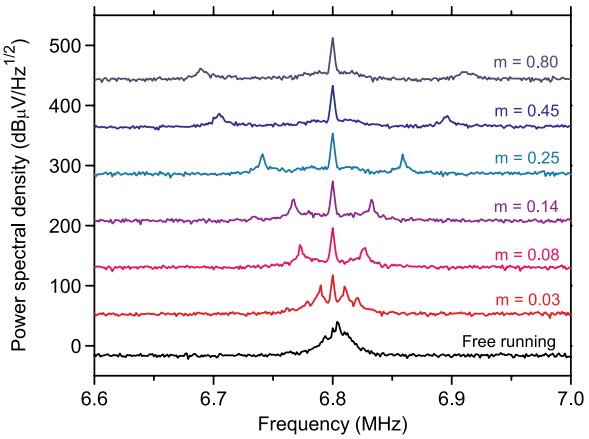

FIG. 4 (color online). Measured rf power spectral density of the detector output with a free running oscillator (black) and oscillations in the presence of an increasingly larger modulation depth of the pump (red to dark blue) for constant *average* power. The curves are offset for clarity.

the OMO to the external clock. Interestingly, sidebands appear again. A prominent feature is that the location of the sidebands is not constant: the offset frequency increases with m. All of this is reproduced in the numerical simulations [13], showing that many of the phenomena observed in the two-OMO case can also be understood in the conceptually simpler injection-locking experiments [26].

Our technique of coupling mechanical oscillators via a single photonic bus creates a whole new platform for nonlinear studies. It will enable synchronization of large arrays of individual optomechanical elements with interesting new collective phenomena [27] and allows synchronization over arbitrarily long distances. Finally, by exploiting the memory storage capabilities of the double well resonators we envision combining the information of the mechanical bits with synchronization. This could, for example, be used to perform conditional coupling of oscillators, an interesting future direction enabled by our cavity field coupling.

We acknowledge funding support from a STIR grant from ARO and DARPA/MTO's ORCHID program through a grant from AFOSR. M. P acknowledges a Rubicon fellowship from the Netherlands Organization for Scientific Research (NWO)/Marie Curie Cofund Action. F. M. acknowledges an ERC Starting Grant, ITN cQOM, and a DFG Emmy-Noether grant. H. X. T. acknowledges support from a Packard Fellowship in Science and Engineering and a Career Grant from the National Science Foundation. The authors thank Dr. M. Rooks of the Yale Institute for Nanoscience and Quantum Engineering for helping with the e-beam lithography, and Michael Power for helping with device fabrication. M. B. and M. P. contributed equally to this work.

*To whom all correspondence should be addressed.
hong.tang@yale.edu

[1] J. Kurths, A. Pikovsky, and M. Rosenblum, *Synchronization: A Universal Concept in Nonlinear Sciences* (Cambridge University Press, Cambridge, England, 2001).
[2] K. S. Thornburg, M. Möller, R. Roy, T. W. Carr, R.-D. Li, and T. Erneux, Phys. Rev. E **55**, 3865 (1997).
[3] J. J. Lynch and R. A. York, IEEE Microwave Guid. Wave Lett. **5**, 213 (1995).
[4] A. B. Cawthorne, P. Barbara, S. Shitov, C. Lobb, K. Wiesenfeld, and A. Zangwill, Phys. Rev. B **60**, 7575 (1999); H. S. J. van der Zant and R. Fazio, Phys. Rep. **355**, 235 (2001).
[5] A. Slavin, Nat. Nanotechnol. **4**, 479 (2009).
[6] S. H. Strogatz, Physica (Amsterdam) **143D**, 1 (2000).
[7] C. Huygens (Hugenii), *Horologium Oscillatorium* (Apud F. Muguet, Parisiis, France, 1673) [*The Pendulum Clock* (Iowa State University Press, Ames, 1986)].
[8] J. L. Arlett, E. B. Myers, and M. L. Roukes, Nat. Nanotechnol. **6**, 203 (2011).
[9] X. L. Feng, C. J. White, A. Hajimiri, and M. L. Roukes, Nature Nanotech. **3**, 342 (2008).
[10] R. Lifshitz, E. Kenig, and M. C. Cross, in *Fluctuating Nonlinear Oscillators: From Nanomechanics to Quantum Superconducting Circuits*, edited by M. I. Dykman (Oxford University Press, Oxford, 2012), Chap 11; M. C. Cross, A. Zumdieck, R. Lifshitz, and J. L. Rogers, Phys. Rev. Lett. **93**, 224101 (2004).
[11] C. A. Holmes, C. P. Meaney, and G. J. Milburn, Phys. Rev. E **85**, 066203 (2012).
[12] M. Zhang, G. S. Wiederhecker, S. Manipatruni, A. Barnard, P. McEuen, and M. Lipson, Phys. Rev. Lett. **109**, 233906 (2012).
[13] See Supplemental Material at http://link.aps.org/supplemental/10.1103/PhysRevLett.111.213902 for device charactization, and details of the model and numerical simulations.
[14] G. Heinrich, M. Ludwig, J. Qian, B. Kubala, and F. Marquardt, Phys. Rev. Lett. **107**, 043603 (2011).
[15] M. Bagheri, M. Poot, M. Li, W. P. H. Pernice, and H. X. Tang, Nature Nanotech. **6**, 726 (2011).
[16] K. J. Vahala, Phys. Rev. A **78**, 023832 (2008).
[17] M. Hossein-Zadeh and K. J. Vahala, IEEE J. Sel. Top. Quantum Electron. **16**, 276 (2010).
[18] Q. Lin, J. Rosenberg, X. Jiang, K. J. Vahala, and O. Painter, Phys. Rev. Lett. **103**, 103601 (2009); S. Tallur, S. Sridaran, and A. Bhave, Opt. Express **19**, 24 522 (2011).
[19] T. J. Kippenberg and K. J. Vahala, Science **321**, 1172 (2008); M. Poot and H. S. J. van der Zant, Phys. Rep. **511**, 273 (2012).
[20] C. H. Metzger and K. Karrai, Nature (London) **432**, 1002 (2004).
[21] A. Hajimiri and T. Lee, *The Design of Low Noise Oscillators* (Kluwer Academic, Dordrecht, 1999).
[22] T. J. Johnson, M. Borselli, and O. Painter, Opt. Express **14**, 817 (2006).
[23] F. Marquardt, J. G. E. Harris, and S. M. Girvin, Phys. Rev. Lett. **96**, 103901 (2006).
[24] M. Poot, K. Y. Fong, M. Bagheri, W. H. P. Pernice, and H. X. Tang, Phys. Rev. A **86**, 053826 (2012).
[25] In the experiments, the optomechanical coupling is displacement dependent and due to the asymmetry in the double-well potential there is a much larger frequency difference.
[26] M. Hossein-zadeh and K. J. Vahala, Appl. Phys. Lett. **93**, 191115 (2008); M. Zalalutdinov, K. L. Aubin, M. Pandey, A. T. Zehnder, R. H. Rand, H. G. Craighead, J. M. Parpia, and B. H. Houston, Appl. Phys. Lett. **83**, 3281 (2003).
[27] M. Ludwig and F. Marquardt, Phys. Rev. Lett. **111**, 073603 (2013).